PRELIMINARY RESULTS OF THE XSAT IN-ORBIT IRIS CALIBRATION AND VALIDATION CAMPAIGN

Wee Juan TAN[1], Kim Hwa LIM[1] and Leong Keong KWOH[2]

[1]Reseach Scientist, Centre for Remote Imaging, Sensing and Processing, National University of Singapore
Block S17 Level 2, 10 Lower Kent Ridge Road, Singapore 119076
Tel: +65-65165571
Email: crstwj@nus.edu.sg

[2]Director, Centre for Remote Imaging, Sensing and Processing, National University of Singapore
Block S17 Level 2, 10 Lower Kent Ridge Road, Singapore 119076

KEY WORDS: MTF, Radiometric Calibration, Validation, XSAT, Normalization

ABSTRACT:

XSAT, a Singapore built Earth Earth Observation microsatellite was placed in polar orbit on 20th April 2011 and has completed its LEOP phase. It has now begun its primary mission of earth observation. The main EO payload is IRIS, a multispectral camera with red, green and near infrared bands and a specified ground sample distance of 10m. This paper describes the process of calibration and validation of IRIS. Two aspects of camera performance are examined: 1) The Modular Transfer Function (MTF) has been estimated with the sharp linear edge method. A man-made high contrast linear edge at the Pasir Panjang terminal has been selected to be the target object. From the target, an Edge Spread Function (ESF) is estimated by interpolating the image appropriately. The MTF is then obtained by differentiating the ESF. 2) Inter-pixel normalization. Sensors left without normalization would exhibit a visible amount of inter pixel variation for any given uniform illumination. This results in visible along-track striations. Normalization is the process of adjusting the individual pixel responses in order to minimize inter pixel variation. In this paper we present the process used to normalize pixel responses.

1. XSAT IRIS Calibration and Validation Campaign

1.1 Overview of IRIS

XSAT, a Singapore built Earth Observation microsatellite was placed in polar orbit on 20th April 2011 and has completed its LEOP phase. It has now begun its primary mission of earth observation. The main EO payload is IRIS, a multispectral camera with red, green and NIR bands. This paper describes the process of calibration and validation of IRIS. Two aspects of camera performance are examined: 1) The Modular Transfer Function (MTF) 2) Inter-pixel normalization or de-striping.

2. IRIS Modulation Transfer Function Estimation

2.1 Introduction

The determination of MTF is based on the linear edge method [1]. The linear edge method is to estimate the Point Spread Function (PSF) from differentiating the Edge Spread Function (ESF) obtained from a man made linear object on the ground.

2.2 MTF Results

The data set that we used is acquired on May 20, 2011 over the Singapore. The linear target that we selected for the MTF estimation is at the Pasir Panjang Harbour terminal as shown in Fig. 1. The linear edges in the red and green rectangles are used to determine the along track and across track MTF respectively.

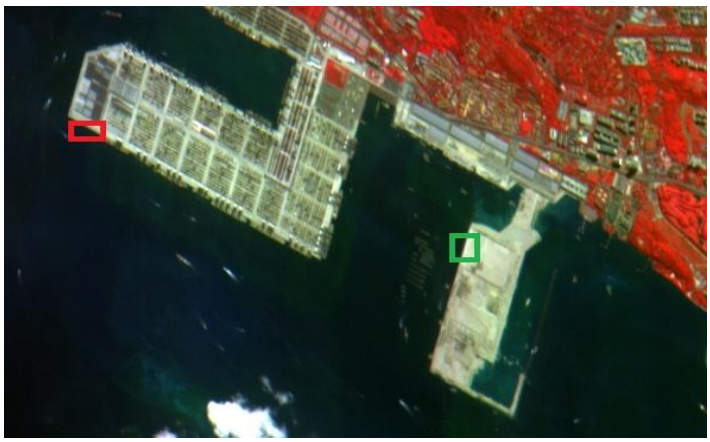

Fig. 1. The Pasir Panjang Harbour terminal selected for the MTF linear edges. The linear edge in the red rectangle is for determining along track MTF and the one in the green rectangle is for across track MTF.

To determine the linear edges, we find the exact edge locations line by line. The exact edge locations are at the maximum slope of the line profiles. Once the edge locations are determined, we fitted them with a straight line as shown in Fig. 2 (a). With the straight line edge, we formed an Edge Spread Function (ESF) by determining the sub-pixel values on the straight edge. The ESF is shown in Fig. 2 (b).

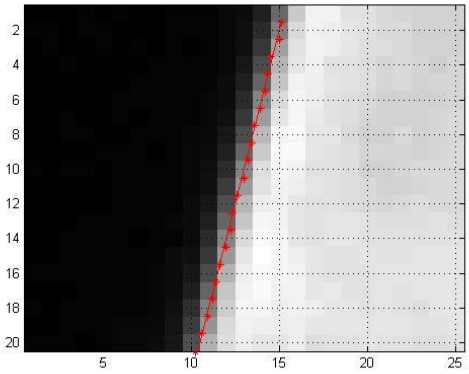

Fig. 2 (a) A straight line is fitted from the edge locations.

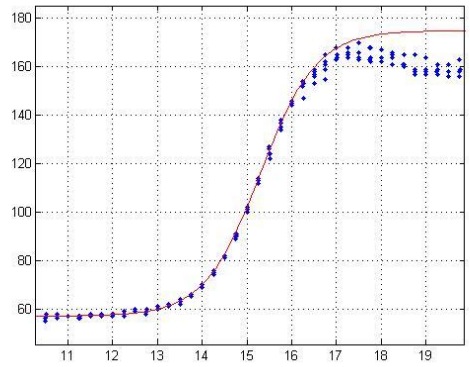

Fig. 2 (b) The Edge Spread Function

The ESF curve is then fitted with an analytical function with formula 1/(1+exp(-a*t)). The Point Spread Function (PSF) is obtained by differentiating the ESF fitted function as shown in Fig. 3 (a). The Modular Transfer Function (MTF) is Fourier transformed from the ESF as shown in Fig. 3 (b). The results for the along track are shown in Fig. 4.

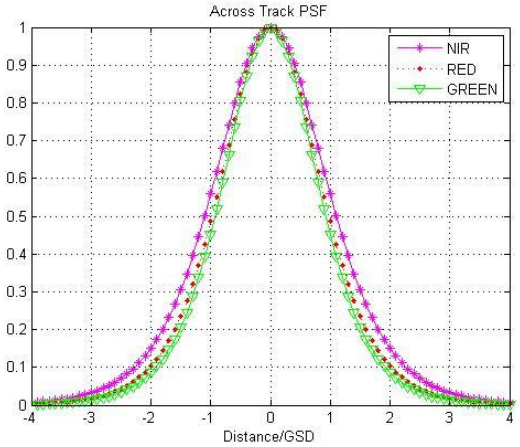

Fig. 3 (a) Across Track Point Spread Functions for each bands.

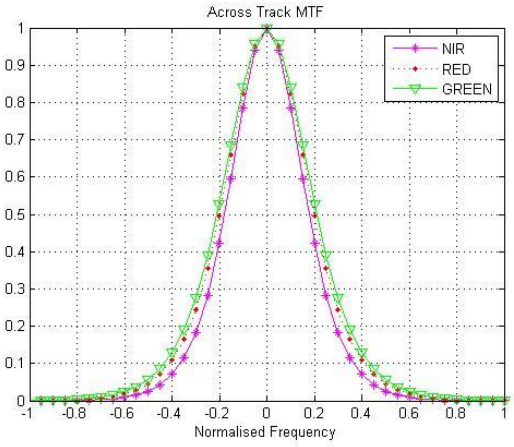

Fig. 3 (b) Across Track MTF for each bands.

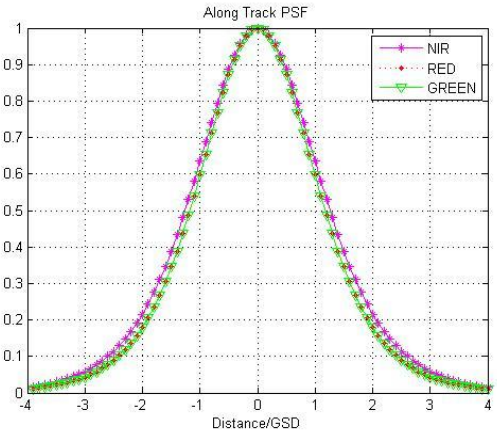

Fig. 4 (a) Along Track Point Spread Functions for each bands.

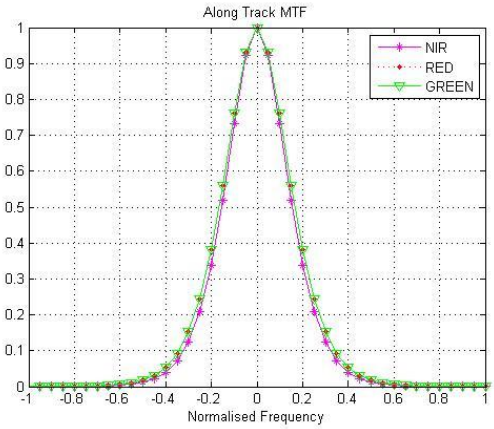

Fig. 4 (b) Along Track MTF for each bands.

2.3 MTF Conclusions

The MTF at Nyquist for all bands for both along track and across track are less than 10%. These results are much less than the NTF specifications given by the vendor, which is more than 15%. The degradation in the MTF may be due to the fact that the sensor is operating at a lower temperature (6^{o}C) than what it should have (20 ^{o}C).

3. Relative Normalization

Individual sensor elements in the IRIS sensors are CCDs with the usual variations in responses typical for such devices. To remove visible striping, relative normalization is performed. An uncorrected image will exhibit vertical striations as can be seen in Fig. 5.

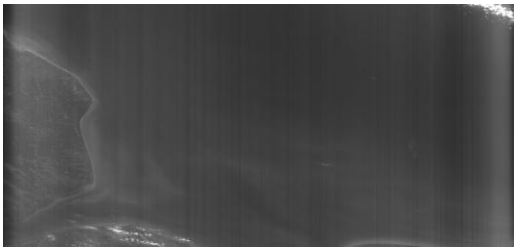

Fig. 5. Uncorrected IRIS Image

3.1 Methodology

To more thoroughly understand the nature of the striping, data from three months of imaging is examined. If we assume that over time, each sensor element is exposed to identical distributions of radiances, the shape of the cumulative distribution function for each sensor element should be identical. Fig. 6. shows the cumulative histogram of relative frequencies of digital numbers for all the sensor elements. In this figure, it can be seen that striations are highly visible. If the underlying assumption of identical distribution of radiance holds, it can be surmised that the striations are due to differences in sensor element responses to any given radiance value.

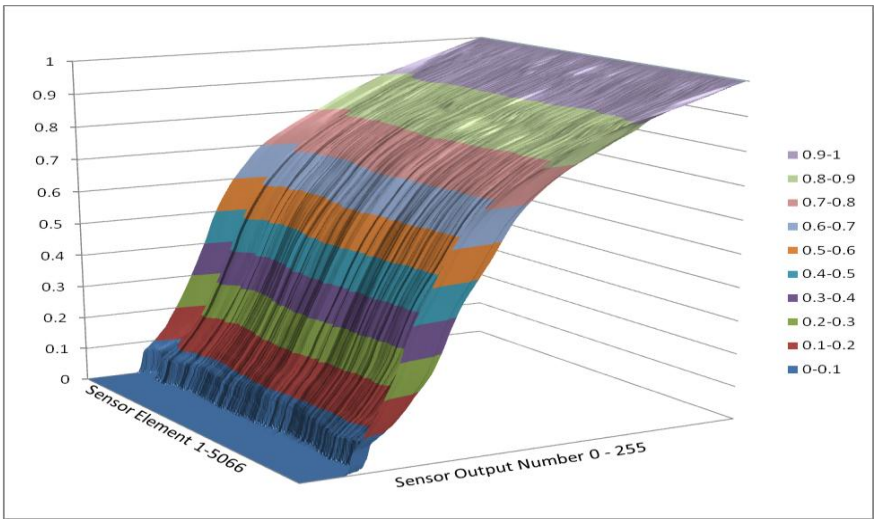

Fig. 6. Cumulative histogram of relative frequencies of sensor values captured over the months of May, June and July.

Two approaches were attempted to perform relative normalization. In the uniform target approach, an area target with highly uniform appearance and whose illumination during

the day is not too bright is selected. The pixels along track are all averaged up, and the deviations are extracted to form the correction dataset. In the second method, the cumulative histogram of each sensor element is matched to a reference histogram. The methods are detailed in the following sections.

3.1.1 Uniform Target Method

In this exercise, a long, cloud free image of South China Sea was captured and the digital numbers averaged alongtrack. The attitude at capture was nadir pointing to minimize uneven illumination due to solar incident angle differences across track.

By averaging over many lines, any inter-line noise and variations in sea surface illumination is removed, allowing the interpixel variation to be extracted. The distribution of the pixel values over the uniformly lit image is shown in Fig. 7.

The global average, μ, of the entire image is found, and the following formula is used to extract the gain correction coefficients.

Fig.7. Histogram of reference uniform target image.

$$\gamma_i = \mu / Y_i$$

where γ_i is the gain co-efficient for sensor element *i*, and Y_i is the mean digital number from sensor element *i* over the entire uniform image. To apply this gain co-efficient to subsequent images the following formula is used:

$$Y'_i = \gamma_i \times Y_i$$

where Y'_i is the corrected digital number for sensor element *i*.

3.1.2 Matched Cumulative Histogram Method

With a large enough collection of images, the distribution of radiances each sensor element is exposed to should be identical. Any deviations between the distributions can then be attributed to the differences in responses between sensor elements. These differences can then be extracted, and a look up table formed to tabulate the differences. Since prior knowledge of the scene radiances is unavailable, this method cannot be used for absolute calibration. However, if a carefully selected sensor element (or element group) can be used as a reference, relative normalization of any arbitrary sensor element with respect to it can be made. Suppose a sensor element *i* is exposed to a distribution of scene radiances, and responds with output x_i. The histogram of counts for sensor element *i* is then $p_i(x)$. The cumulative histogram of relative frequencies can then be calculated:

$$P_i(x) = \sum_{t=0}^{x} p_i(t)$$

This is a monotonically increasing function of *x*, with a maximum value of 1.0. Given a reference cumulative histogram $P_r(x)$, it stands to reason that there will a matching value such that

$$P_r(x') = P_i(x)$$

where *x'* is the normalized value of *x*. Finding the inverse of the reference cumulative histogram would then yield the desired corrected output.

$$x' = P_r^{-1}(P_i(x))$$

This will always hold true if both the reference and the arbitrary cumulative histograms are monotonically increasing, as would be the case for a regular CCD sensor. Fig. 8. shows the relationship between the reference cumulative histogram and the histogram of the channel to be normalized, in this case, sensor element 5054.

To perform correction of sensor element 5054, the equivalent digital number of the reference channel for each digital number of sensor element 5054 is found. In this example, sensor element outputs value 89, corresponding to a cumulative histogram value of 0.58. The inverse of the reference cumulative histogram at 0.58 is 101. Since the closed form solution of the reference is not available, this is done using a simple iterative search in a software program. A table entry then holds value 101 for a lookup value of 89. This process is repeated for each level of

output, and for each of the 5066 sensor elements. To construct the reference histogram for IRIS, the cumulative histogram of sensor values for sensor indices 3000 to 3999 is averaged. This differs from the paper by Horn and Woodham [2], who used the average of the entire image as the reference histogram to normalize LANDSAT images. This also differs from the implementation by Weinreb et al [3], who selected a single channel for destriping GOES images. This is because, upon examination of the histograms from IRIS, it appears that there may be some low frequency correlated errors at the sides of the images possibly be due to light leakage. By using sensor elements from the middle segment of the sensor array, this is largely avoided.

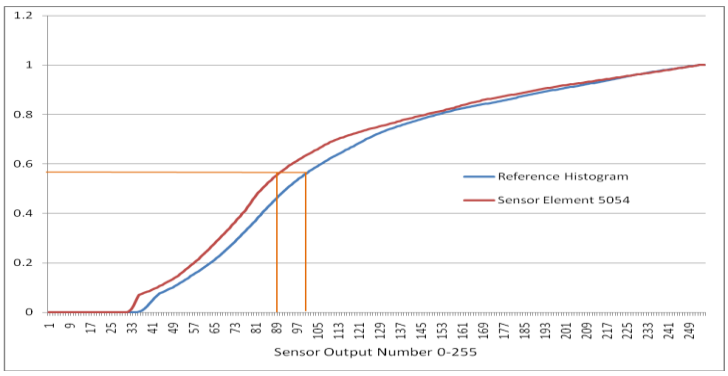

Fig. 8. Reference cumulative histogram and cumulative histogram for sensor element 5054.

3.2 Results of Relative Normalization Procedure

To provide a clearer picture of the improvements, the cumulative histogram of sensor output numbers for all the scenes in May, June and July are shown, post-correction is shown in Fig. 9 (a) and Fig. 9 (b).

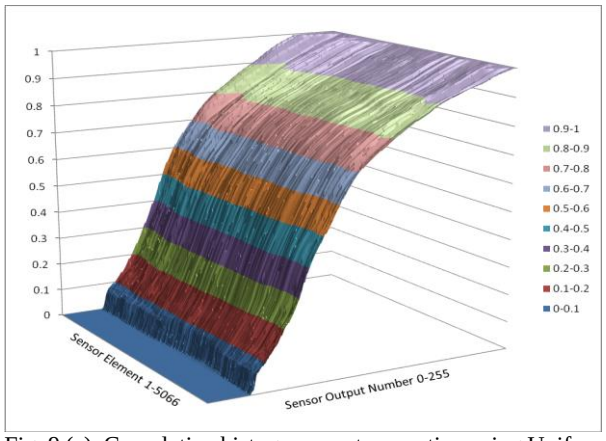

Fig. 9 (a). Cumulative histogram post correction using Uniform Target method.

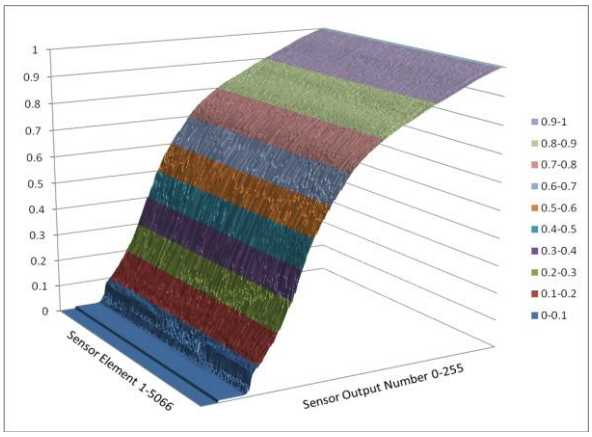

Fig. 9 (b). Cumulative histogram post correction using Matched Histogram method.

It is clear from the post correction cumulative density diagram that some improvement has been effected by the corrective procedure. However, it can also be seen that the higher brightness regions of the images are less well corrected than the lower and mid-tone regions. This could be due in part to the correction data coming mainly from an image with lower levels of illumination.

The results for the matched cumulative histogram technique show more consistent cumulative histograms across the sensor elements, at all illumination levels. This in itself does not mean de-striping was successful, as it is predicate upon the underlying assumption that the sensor elements were all exposed to a sufficiently large sample set.

To verify the performance of the correction algorithms, images from both low and high illumination levels are examined. The real world results are shown in Fig. 10.

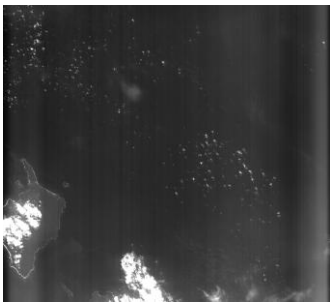

Fig. 10 (a). Uncorrected, low brightness.

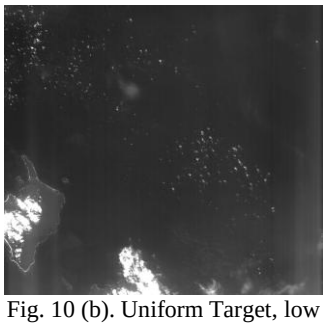

Fig. 10 (b). Uniform Target, low brightness.

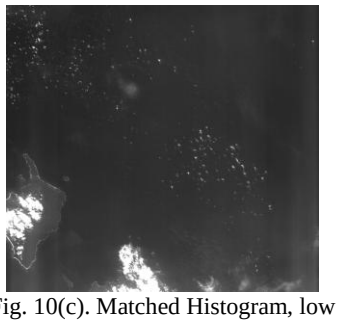

Fig. 10(c). Matched Histogram, low brightness.

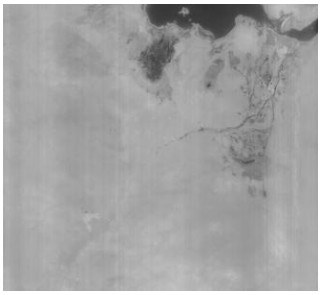

Fig. 10 (d). Uncorrected, high brightness.

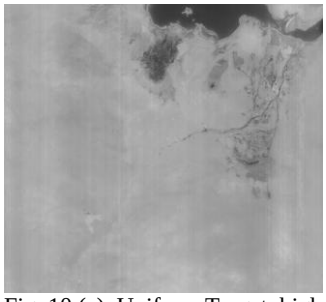

Fig. 10 (e). Uniform Target, high brightness.

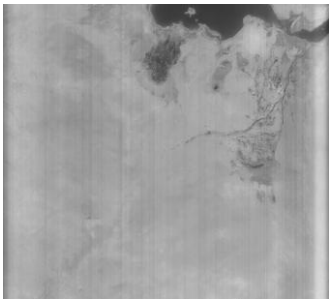

Fig. 10 (f). Matched Histogram, high brightness.

It can be seen that, at lower levels of illumination, both correction techniques made some improvement, with the matched histogram method showing a better overall improvement. At high levels of illumination, neither algorithm performs adequately, with the matched histogram method showing signs of over and under correction. A possible cause is inadequate data at the high brightness portion of the histogram, resulting in sensor elements not being exposed to the same histogram. To determine if this was the case, a difference map between the matched histogram output and uncorrected image was constructed by subtracting the pixels of one image from the other, then mapping negative numbers to red and positive numbers to green. This allows us to see the gross structure of the mis-corrections. If inadequate data were the cause, the difference map would show red / green areas on subject level scales (ie, large cloud size, land mass size). As can be seen in Fig. 11, the structure of the mis-correction is in the order of hundreds to thousands of sensor elements wide. This is compatible with the hypothesis that different portions of the sensor were exposed to different histograms especially at the high brightness levels. This is inline with empirical observations that tropical land and ocean images, which make up the bulk of the images, cover the low to mid brightness portion of the histogram. Thus we can conclude that inadequate data was present in the higher levels of brightness for the effective use of matched cumulative histogram method.

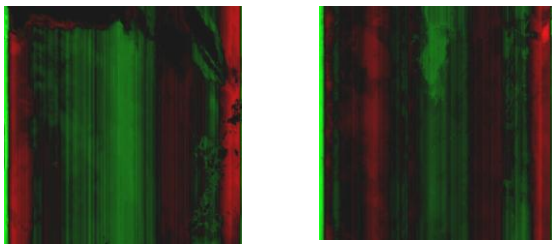

Fig. 11 (a+b) Map of brightness differences between uncorrected and matched histogram corrected images.

4 Conclusion and Future Work

XSAT has started its main work of earth observation and CRISP will monitor the performance of the IRIS payload over time. Periodic relative normalization will be carried out, with further studies made to ascertain the efficacy of various relative normalization techniques, including matched cumulative histograms with larger data sets, and uniform target with intensity segmented datasets. MTF assessments may be carried out again if onboard thermal conditions are revised.

5 References

1. R. Ryan, B. Baldridge, R. A. Schowengerdt, T. Choi, D. L. Helder, S. Blonski. 2003. *IKONOS spatial resolution and image interpretability characterization.* Remote Sensing Environment 88 (2003), 37-53

2. B. K. P. Horn and R. J. Woodham. 1979. *Destriping LANDSAT MSS Images by Histogram Modification.* Computer Graphics and Image Processing 10, 69-83.

3. M. P. Weinreb, R. Xie, J. H. Lienesch, and D. S. Crosby. 1989. *Destriping GOES Images by Matching Empirical Distribution Functions.* Remote Sensing of the Environment. 29:185-195.